

# Transporting fibres as reinforcement in self-compacting concrete

Steffen Grünewald, Joost C. Walraven

Department of Design and Construction, Delft University of Technology, the Netherlands

The development of self-compacting concrete (SCC) was an important step towards efficiency at building sites, rationally producing prefabricated concrete elements, better working conditions and improved quality and appearance of concrete structures. By adding fibres to SCC bar reinforcement can be replaced and the performance of concrete structures enhanced. Self-compacting fibre reinforced concrete (SCFRC) combines the benefits of SCC in the fresh state and an enhanced performance of fibre reinforced concrete in the hardened state. With the special characteristics of SCFRC new fields of application can be explored.

This paper describes results of a PhD-study [Grünewald, 2004], which was carried out at the Delft University of Technology. The effect of steel fibres on the characteristics of SCC in the fresh and the hardened state are discussed. Tools are provided to optimise SCFRC and full-scale case-studies demonstrate the potential of SCFRC.

*Key words: Self-compacting concrete, steel fibres, workability, bending behaviour, orientation*

## 1 Introduction

SCC spreads homogeneously due to its own weight, without any additional compaction energy and does not entrap air. The main characteristics of SCC in the fresh state are filling ability, passing ability and segregation resistance. Fibres have been produced in a wide range of materials, shapes and characteristics. They improve the performance (strength and toughness) of brittle cement-based materials by bridging cracks, transmitting stress across a crack and counteracting the crack growth. The steel fibre is the most common fibre type in the building industry; other fibre types like plastic, glass and carbon fibres contribute with a smaller part to the market. Dependent on the type and the content of the fibres the workability of concrete can be significantly affected. With SCFRC light structures can be designed with lower costs for transport, storage and placement. With fibres concrete becomes more ductile, less material has environmental benefits and more slender structures require less reinforcement. Fibres improve the abrasion and impact resistance; appli-

cations with fibres can be economical and bar reinforcement can be replaced. The production process can be facilitated with SCC. SCFRC can be combined with prestressing strands, used for remote casting, to enhance the fire resistance, to obtain smaller crack widths and to improve the durability.

Composing SCFRC with defined performance in the fresh and the hardened state is a complex task; several design tools are described in this paper. SCFRC can be optimised for various purposes: to apply the highest possible fibre content, to obtain the best performance-cost ratio, to design the granular skeleton for the highest packing density and/or to produce concrete with the lowest possible costs.

## 2 SCFRC in the fresh state

### **The effect of fibres on workability**

Fibres affect the characteristics of SCC in the fresh state. They are needle-like particles that increase the resistance to flow and contribute to an internal structure in the fresh state. Steel fibre reinforced concrete is stiffer than conventional concrete. In order to optimise the performance of the single fibres, fibres need to be homogeneously distributed; clustering of fibres has to be avoided. The effect of fibres on workability is mainly due to four reasons: First, the shape of the fibres is more elongated than the aggregates; the surface area at the same volume is higher. Second, stiff fibres change the structure of the granular skeleton, whereas flexible fibres fill the space between them. Stiff fibres push apart particles that are relatively large compared to the fibre length, which increases the porosity of the granular skeleton. Third, the surface characteristics of fibres differ from that of cement and aggregates, e.g. plastic fibres might be hydrophilic or hydrophobic. Finally, steel fibres often are deformed (i.e. have hooked ends or are wave-shaped) to improve the anchorage between them and the surrounding matrix. The size of the fibres relative to the aggregates determines their distribution (Figure 1). To be effective in the hardened state it is recommended to choose fibres not shorter than the maximum aggregate size [Johnston, 1996; Vandewalle, 1993]. Usually, the fibre length is 2-4 times that of the maximum aggregate size.

### **Packing density**

The disturbing effect of fibres on the packing density is demonstrated in Figure 2 for different sand contents. The packing density (PD) is complementary to the porosity  $P$  (volume of interstices) of the granular skeleton ( $P = 1 - PD$ ). In the experiments, the content

sand (0.125-4 mm) of the total aggregate (coarse aggregates 4-16 mm) was varied from 0-100 Vol.-% and different types and contents of the steel fibres were tested.

The applied fibre content in Figure 2 was 1.5 Vol.-% of the aggregate particles. The higher the aspect ratio (ratio of fibre length to diameter;  $L_f/d_f$ ) and the lower the content of sand the more pronounced is the effect of fibres on the packing density. At sand contents of 75 Vol.-%, about the same packing density was found for different types of steel fibres. The relative size between the fibres and the aggregates affects the packing density. The maximum decreases and shifts towards higher sand contents. In order to compensate for the effect of the fibres the mixture composition has to be adjusted by increasing the content of grains that are relatively small compared to the fibre length (cement, filler and/or small aggregate grains).

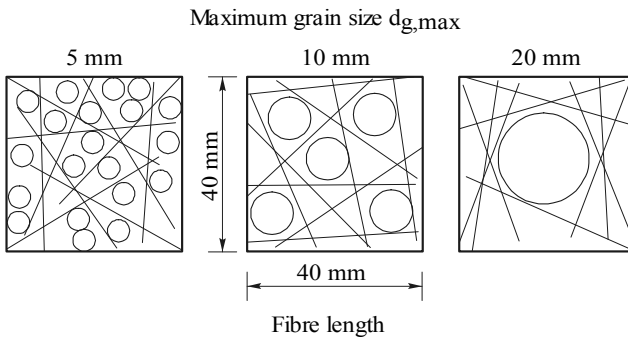


Figure 1: Effect of the aggregate size on the fibre distribution [Johnston, 1996]

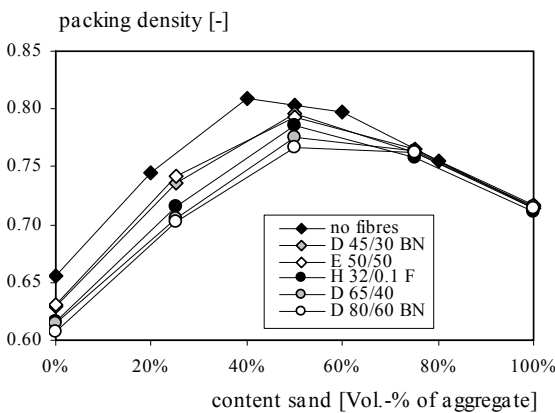


Figure 2: Effect of the sand content and the type of the steel fibres (at 1.5 Vol.-%) on the packing density (fibre type, first index:  $L_f/d_f$ )

### Optimisation of the mixture composition

Parameter studies were performed in order to answer the question to which degree characteristics of SCC in the fresh state are affected and whether the mixture composition has to be different and if so, how to compose it for optimised SCFRC. The more fibres are added and the higher is their aspect ratio, the more the slump flow [description of this test: Bartos et al., 2000] decreases compared to a reference SCC without fibres. The fibre factor ( $V_f \cdot L_f / d_f$ ) is the product of the volume of the steel fibres times the aspect ratio and was applied to compare the effect of different types and contents of the steel fibres on the slump flow. As an example, Figure 3 shows the results of the mixtures of series OS3, OS4 and OS8 [Grünewald, 2004].

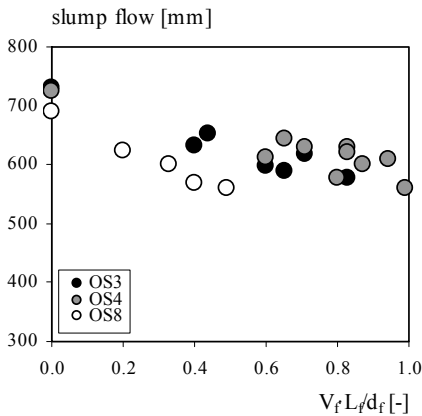


Figure 3: Effect of the fibre factor and the mixture composition on the slump flow of mixtures of series OS3, OS4 and OS8

For high fibre contents the slope (Figure 3: the decrease of slump flow at increasing fibre factor) of an optimised SCC for fibres should be as low as possible, whereas the slump flow of the reference mixture without fibres should be as large as possible. The segregation of the fibres has to be avoided by providing sufficient segregation resistance. The mixture composition of SCFRC can be optimised by considering the following principles:

- To initiate the flow a minimum shear stress (yield value) has to be surpassed. Beyond this threshold, the shear stress is linearly related (with plastic viscosity being the slope) with the increase of the rate of deformation. Fibres increase the yield value (Figure 4) and the plastic viscosity (Figure 5) of SCC. The effect of fibres depends on the composition and characteristics of SCC in the fresh state. In order to obtain a con-

crete with fibres that is self-compacting their effect has to be compensated for. High filling ability and sufficient segregation resistance often are irreconcilable demands for SCC, which only leaves a small range within which SCC is self-compacting. Depend-ent on the fibre type and the mixture composition, the fibre dosage for SCC is limited.

- The packing density has to be optimised to increase the surplus of paste in excess to fill the interstices of the aggregates. The range of aggregates has to be as wide as pos-sible to increase the packing density of the granular skeleton.
- Coarse (relative to the fibre length) aggregates decrease the maximum possible fibre content and increase the bar spacing required to avoid blocking.

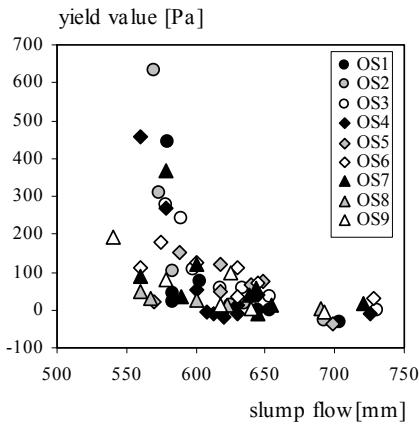


Figure 4: Rheological measurements on SCFRC (series OS1-9): slump flow versus yield value

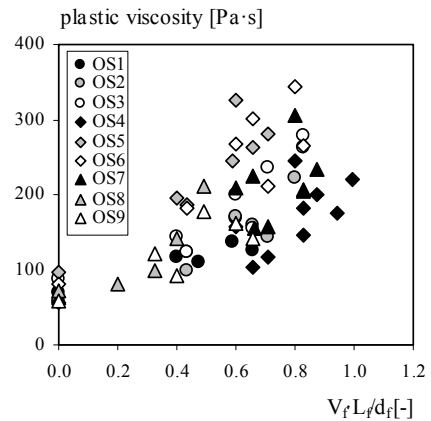


Figure 5: Effect of the fibre factor and the mixture composition on the plastic viscosity (series OS1-9)

### Maximum fibre content

The maximum fibre content, at which a self-compacting concrete can be produced, de-pends on the fibre type, the mixture composition, the mixing process and the characteris-tics of the concrete in the fresh state. For plain concrete, the compaction technique also affects this parameter. In order to determine the maximum fibre content of SCFRC, differ-ent series of mixtures were tested and the fibre content was increased in steps of 20 kg/m<sup>3</sup>. The ‘maximum fibre content’ is defined to be the highest possible amount of steel fibres, which can be added to SCC; SCFRC is self-compacting below this fibre content. The follow-ing criteria were applied to determine the maximum fibre content: a slump flow of at least 600 mm and a homogenous distribution of SCC and fibres along the flow (slump flow test).

Three observations of the slump flow (Figures 6-8) indicated that the maximum fibre content was surpassed. Fibre types having a large surface area decrease the flowability of SCC (Figure 6). The fibres are homogeneously distributed but the contour of the flown-out concrete is not round. This flow pattern often corresponds with a flow diameter smaller than 600 mm. Long fibres and/or large aggregates tend to cluster along the flow; the flow diameter is barely affected (Figure 7). Fibre types of intermediate aspect ratios ( $L_f/d_f$ : 45-65) often showed a combination of flow patterns (Figure 8 is a combination of Figure 6 and Figure 7). The free flow is obstructed and a cluster of fibres and/or aggregates remains in the centre of the flow table.

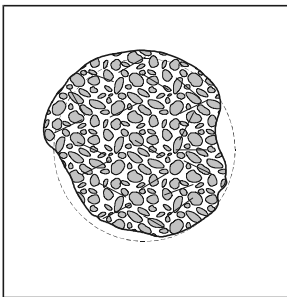


Figure 6: Spread area for fibres having a large surface area (example: Dramix 80/30 BP)

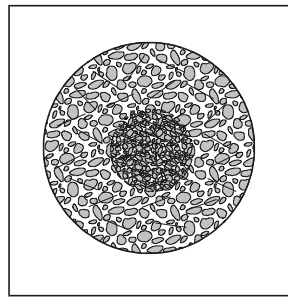


Figure 7: Spread area for long fibres (example: Dramix 80/60 BP)

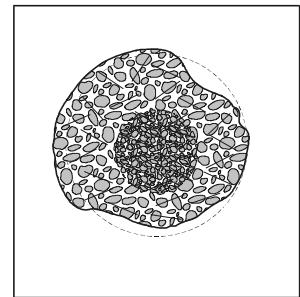


Figure 8: Spread area for fibres having a low to intermediate aspect ratio (example: Dramix 65/40 BN)

### Prediction of the maximum fibre content

The ability of concrete to pass reinforcement bars without blocking is defined as passing ability. The passing ability of SCC can be predicted by calculating the risk of blocking [Bui, 1994; Petersson et al., 1998], which takes into account the size, the shape (nature or crushed) and the distribution of the aggregates. Figure 9 shows the relative effect of the aggregates on the passing ability of SCC ( $n_{abi}$ ) related to the ratio of the bar spacing  $c$  divided by the diameter of the equivalent aggregate particle diameter  $D_{af}$ . The bar spacing  $c$  is the opening between the rebars of the L-box, which is a test method to determine the passing ability of SCC. The equivalent-diameter  $D_{af}$  of an aggregate fraction can be calculated with Equation 1:

$$D_{af} = M_{i-1} + \frac{3}{4} (M_i - M_{i-1}) \quad (1)$$

in which

$M_i$  upper sieve dimension of aggregate [mm]

$M_{i-1}$  lower sieve dimension of aggregate [mm]

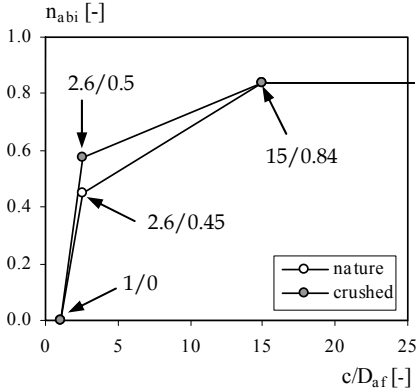


Figure 9: Relation between the ratio of the clear bar spacing  $c$  to fraction diameter of the aggregates and the blocking volume ratio

Similar to the Miner-rule on fatigue, the contribution of each aggregate fraction is accumulated with Equation 2. The 'risk of blocking' has to be smaller than or equal to one. The points of Figure 9 were used for Equation 2 and were determined with an inverse analysis; blocking occurred in the experiments when then risk of blocking was higher than 1.

$$\text{Risk of blocking: } \sum_{i=1}^n \frac{n_{ai}}{n_{abi}} = \sum_{i=1}^n \frac{V_{ai}}{V_{abi}} \leq 1 \quad (2)$$

in which

$n_{ai}$  aggregate contribution of group  $i$  to blocking [-]

$n_{abi}$  blocking volume ratio of group  $i$  [-];  $n_{abi} = V_{abi} / V_t$

$V_t$  total volume of the concrete mix [m<sup>3</sup>]

$V_{ai}$  aggregate volume of group  $i$  [m<sup>3</sup>]

$V_{abi}$  blocking volume of aggregate group  $i$  [m<sup>3</sup>]

A model was developed for SCFRC to predict the maximum fibre factor for fibre lengths in the range of 6-60 mm. The bar spacing to aggregate fraction diameter ratio ( $c/D_{af}$ ) of the

'risk of blocking'- approach was replaced by the ratio of the fibre length to aggregate fraction diameter ( $L_f/D_{af}$ ). The characteristic points of the 'nature' line (Figure 9) were altered to obtain the best correlation with the experimental maximum fibre factors. Figure 10 shows the relation between the ratio fibre length to aggregate diameter and  $n_{a,mfi}$  (MFC-ratio is the relative effect ( $n_{a,mfi}$ ) of aggregates on the maximum fibre content). Relatively large aggregates ( $L_f/D_{af} < 1.8$ ) result in a lower MFC-ratio;  $n_{a,mfi}$  is approximately constant at higher ratios of  $L_f/D_{af}$ .

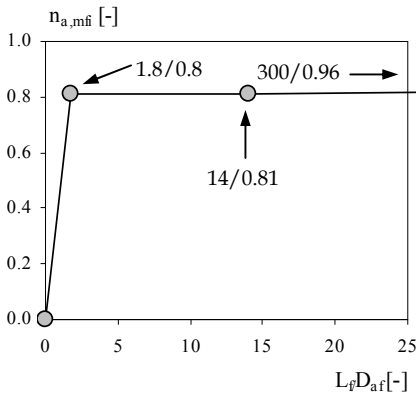


Figure 10: Relation between the ratio fibre length to aggregate diameter and the MFC-ratio ( $n_{a,mfi}$ )

Figure 11 shows the maximum fibre factor of mixtures of different series compared to the maximum fibre content volume (MFC) of the aggregates. The fibre length is the weighted average in case a hybrid mixture of short fibres (6 and 13 mm). The maximum fibre factor ( $V_f \cdot L_f/d_f$ ) can be determined with the MFC-volume as the intersection of the regression line (Equation 3).

$$\text{Maximum fibre factor} = \frac{0.781 - MFC}{0.211} \quad (3)$$

in which MFC is the maximum fibre content volume [-]

SCC is self-compacting at a given fibre factor in case the MFC-volume is equal to or lower than the corresponding value on the regression line of Figure 11. The mixture, which was optimised for the production of slender prestressed sheet piles [Tol, 2002], is also included in Figure 11 (mix sheet piles); its maximum aggregate size was 1 mm.

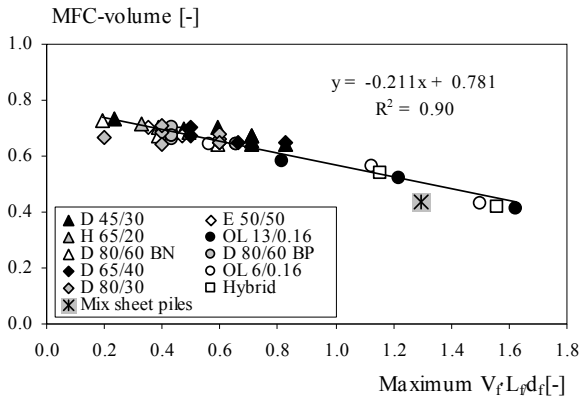


Figure 11: Relation between the maximum fibre factor and the MFC-volume

In order to increase the maximum fibre content the following parameters might be altered: to apply fibres with a lower aspect ratio, to increase the content of cement paste and/or to replace coarse with finer aggregates. Once aggregate fractions with a ratio  $L_f/D_{af}$  smaller than 1.8 are excluded, the paste content becomes the governing parameter.

#### Determination of the required bar spacing

The determination of the minimum bar spacing required to avoid blocking is an essential tool to optimise the mixture composition of SCFRC. A J-ring with seventy-two drilled holes (diameter of the smooth bars: 16 mm) was used to vary the distance of the bars. Blocking is defined to occur in case the difference between the heights of the concrete directly in- and outside the J-ring ( $\Delta h$ ) is at least 10 mm. The bar spacing of the J-ring was varied three times in order to obtain one height difference above and below the criterion for blocking (10 mm). Experiments indicated that the bar spacing of SCFRC has to be increased compared to SCC since the fibres are usually the largest components. Several self-compacting mortars with short steel fibres (6 and/or 13 mm) were tested and are able to pass the J-ring test [Bartos et al., 2000] at a bar spacing of 36 mm without blocking. In contrast, the bar spacing required to avoid blocking of mixtures with long steel fibres might be 99 mm or larger. The 'non-blocking' bar spacing of SCFRC, which was determined from tests with the J-ring, is normalised to the fibre length to generalise the relation. A linear regression line (Equation 4) is applied to determine the 'safe' bar spacing for SCFRC.

$$BF = 0.607 \cdot \frac{c}{L_f} - 0.857 \quad (4)$$

in which

- $BF$  blocking factor of SCFRC [-]  
 $c$  clear spacing between reinforcement [mm]  
 $L_f$  fibre length [mm]

Figure 12 shows the regression line (Equation 4) compared to the test results; the model predicts 'non-blocking' in each case.

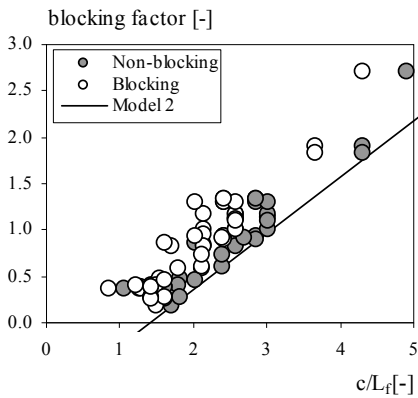


Figure 12: Determination of the bar spacing sufficient for non-blocking compared to the test results of SCFRC

The blocking factor is the product of three parameters that affect the passing ability of SCFRC (Equation 5), which are the risk of blocking, the fibre content and the blocking diameter.

$$\text{Blocking factor (BF)} = BD \cdot V_f \cdot ROB_{(BS)} \tag{5}$$

in which

- $ROB_{(BS)}$  risk of blocking (depends on the chosen bar spacing) [-]  
 $V_f$  fibre content (volume) [Vol.-%]  
 $BD$  blocking diameter (depends on fibres' diameter) [-]

The parameter  $BD$  (Equation 6 relates the dimensionless parameter  $BD$  and  $d_f$ , with  $d_f$  in mm) was applied to characterise different fibre types. The effect of the fibres on the passing ability increased at decreasing diameter. Figure 13 shows the relation between the diameter of the steel fibres and the factor  $BD$ .

$$\text{Blocking diameter (BD)} = 0.553 \cdot d_f^{-1.51} \quad (6)$$

in which  $d_f$  is the fibre diameter [mm].

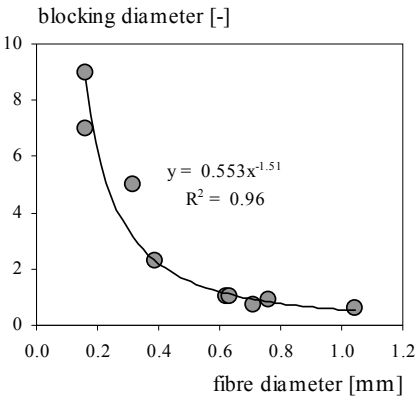


Figure 13: Relation between the diameter of the steel fibres and the blocking diameter ( $BD$ )

The risk of blocking ( $ROB_{(BS)}$ ) has to be determined with the actual bar spacing (Equation 2). As a result, the prediction of the bar spacing is an iterative procedure. The relation proposed (Equation 5) can be applied in two cases: First, in case the design bar spacing is known, the blocking factor can be calculated under consideration of the chosen fibre length. The diameter of the fibre can be calculated from the aspect ratio. The remaining parameters, the fibre volume and the  $ROB$ , might be chosen. The fibre content has to remain below the maximum fibre content. The content and the grading of the aggregates determine the  $ROB$  at this bar spacing. The actual blocking factor has to be smaller than the predicted blocking factor. Second, the model can be applied to calculate the bar spacing required for non-blocking. The blocking factor has to be determined from the mixture composition. In order to calculate the  $ROB$ , the required bar spacing needs to be estimated. A comparison between the estimated and calculated bar spacings is necessary to control the assumed bar spacing.

### 3 SCFRC in the hardened state

#### Improved performance of SCFRC

Steel fibres improve the performance of SCC in the hardened state. The microstructure around the fibres, the distribution and the orientation of the fibres can be rather different in SCC and conventional concrete. In order to design SCFRC, the fibre content has to remain below the maximum fibre content; in SCFRC each fibre is fully embedded in the matrix. In an extended experimental program, the bending behaviour, the single fibre pull-out response of SCFRC and the effect of the production on the orientation of the fibres were studied. Deformation-controlled three-point bending tests with notch were carried out in order to quantify the effect of the fibres on the post-cracking behaviour of SCFRC.

Remarkable differences of the bending strengths and the variation of the results were found between two C55/67 mixtures, one of which was self-compacting and one was cast with conventional steel fibre reinforced concrete [Kooiman, 1998] and which both contained Dramix 80/60 BP steel fibres (fibre content:  $60 \text{ kg/m}^3$ ). Figure 14 shows the results of the bending tests (beam length/width/height: 500/150/150 mm). The average flexural tensile strength of SCFRC at the maximum was 13.5 MPa. The rate of deformation in the study of Kooiman was  $1 \text{ }\mu\text{m/s}$  up to a displacement of 5 mm and  $50 \text{ }\mu\text{m/s}$  beyond 5 mm (SCFRC: constant  $50 \text{ }\mu\text{m/s}$ ). Referring to a study of Gopalaratnam & Shah [1986], a minor influence of this difference on the maximum flexural load can be expected.

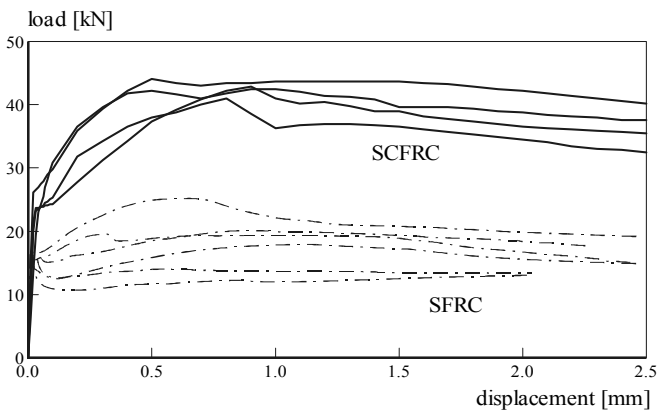


Figure 14: Test results of three-point bending tests: SCFRC versus SFRC

In order to determine the origin of the differences two additional studies were performed: First, the orientation number of the cross-section of the beams were determined with an image analysis. The fibres in SCFRC were more favourably aligned in the direction of the flow; the longer the fibres the higher was the orientation number. Second, a comparison between the pull-out behaviour of single fibres from SCC and conventional concrete showed that in most cases higher pull-out forces were obtained with SCC. In order to design SCFRC, the fibre content has to remain below the maximum fibre content and, as a consequence, each fibre is fully embedded in the matrix. The photographs of the cross-sections of the beams showed that only a few fibres were connected. The variation of bending response is not a material characteristic but also depends on the segregation resistance of SCFRC or steel fibre reinforced concrete and the reproducibility of the production process.

### **Inverse modelling procedure**

The stress-crack width relation can be recalculated from the bending test with an inverse analysis. The inverse modelling procedure consists of four parts: the input level, the numerical level, the accuracy check and the output level [Roelfstra & Wittman, 1986]. On the input level material properties and geometrical boundaries have to be set. The analysis is performed on the numerical level under consideration of the geometry of the specimen, the influence length and the material characteristics. It has to be checked on the accuracy level whether the obtained solution solves the problem with sufficient accuracy. The uni-axial tensile behaviour is the result of the output level.

Hordijk [1991] developed the 'multi-layer procedure' to study and to model the behaviour of plain concrete in bending. The following assumptions are part of the procedure: an area of a beam with a defined width consists of a defined number of layers, which are connected by springs. The response of the beam is the sum of the behaviour of all springs. The stress is linearly distributed over the height of the beam. Equilibrium is found in case the sum of the horizontal internal forces is equal to zero; the external load (bending moment) can be calculated from the internal bending moment. The displacement at the notch has to be incrementally increased at each iteration step; a point of the load-displacement curve is obtained by calculating the bending moment. In order to obtain compatibility of strain and crack width, the crack width has to be divided by an influence length, which is a factor that determines the stiffness and the response of the whole system.

### Calibration of the tensile model

Seventeen different SCFRC-mixtures were tested on their bending performance. Based on the experimental results a combined stress-strain/stress-crack width model for SCFRC in tension was developed. The model was calibrated with results of fifteen mixtures, which contained hooked-end steel fibres. A tensile model (Figure 15) was proposed that takes into account the increase of the load after the first crack appeared.

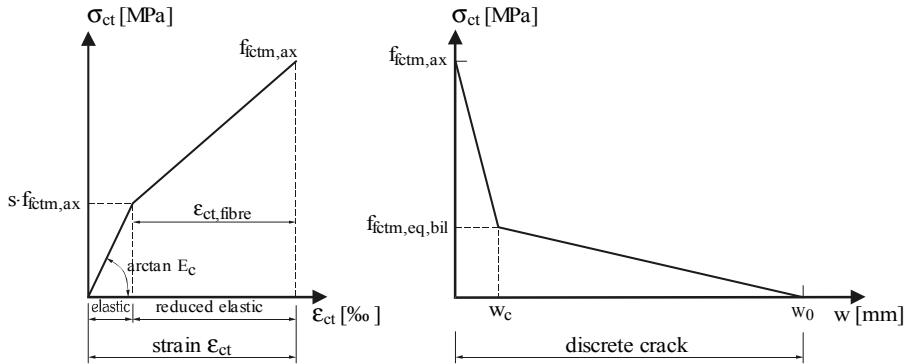


Figure 15: A combined stress-strain/stress-crack width approach for SCFRC in tension (left: stress-strain for the elastic and the reduced elastic phases; right: stress-crack width relation for the softening phase)

The tensile model consists of three parts: one that accounts for the elastic behaviour of the beam, a second that allows to model the reduced elastic regime and a third, which is characterised by a stress-crack width relation. The approach to determine the input parameters was divided into three steps: First, the uni-axial tensile strength ( $f_{ctm,ax}$ ) was varied to fit the experimental maximum flexural load. Second, the post-cracking tail was approximated by varying the equivalent post-cracking strength ( $f_{ctm,eq,bil}$ ), the characteristic ( $w_c$ ) and critical crack widths ( $w_0$ ). Finally, two parameters ( $s \cdot f_{ctm,ax}$  and  $\epsilon_{ct, fibre}$ ) were varied to adequately fit the bending response until the maximum load was reached. Seven input parameters are required to perform the simulation. The following characteristics have to be determined in order to carry out the simulation, which are the E-modulus ( $E_c$ ), the splitting tensile strength with and without steel fibres, the type and the content of the fibres, the orientation number, the packing density of the paste and the water-binder ratio [CUR-recommendation 70, 1999]. Figures 16 and 17 present experimental results and simulations for Dramix 80/60 BP (Figure 16;  $V_f = 60 \text{ kg/m}^3$ ) and Dramix 45/30 BN (Figure 17;  $V_f = 140 \text{ kg/m}^3$ ).

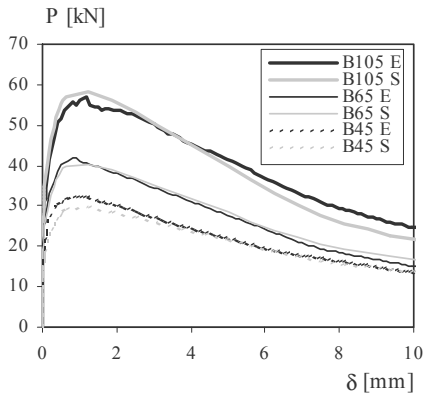


Figure 16: Simulations (S) versus experimental (E) results: effect of the strength class (Dramix 80/60 BP,  $V_f = 60 \text{ kg/m}^3$ )

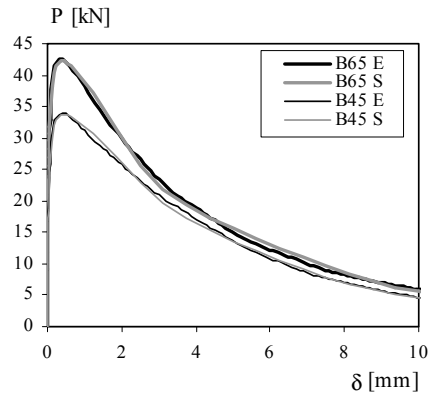


Figure 17: Simulations (S) versus experimental (E) results: effect of the strength class (Dramix 45/30 BN,  $V_f = 140 \text{ kg/m}^3$ )

The input parameters of the model can be calculated with Equations A1-A9 and Table A1 (see Appendix). The difference between results of simulations with the combined tensile model and experimental results (for mixtures with hooked-end steel fibres) are in average smaller than 8% (average maximum flexural load 7.2%; fracture energy: 7.4%).

#### 4 Full-scale applications with SCFRC

Flowable mixtures are preferred in production in order to minimise the effort to compact the concrete. The applicability of SCFRC in practice and the influence of the casting method were determined in three case-studies, which are sheet piles, tunnel segments and large beams.

##### Application: Sheet piles

Sheet piles are ground- and water-retaining structures, which are usually made of steel. Prestressed sheet piles produced with SCFRC have several advantages compared to a standard concrete sheet pile: the placement of the concrete is easier (no bar reinforcement has to be placed), the storage of the segments requires less space, more sheet piles can be transported with one truck (they are lighter and occupy less space) and the placement in the ground is easier (less resistance). Figure 18 shows an innovative sheet pile (produced by SPANBETON) in comparison with a conventional concrete sheet pile; the length of the sheet piles is 12.5 m.



Figure 18: Prestressed sheet piles cast with SCFRC (left: C90/105) and conventional concrete (right: B55/67 concrete with additional bar reinforcement)

An optimised mixture was developed at the Delft University of Technology and fulfilled all design criteria, i.e. a 1-day compressive strength of at least 60 MPa (28 days: C90/105). The mixture was self-compacting and contained 125 kg/m<sup>3</sup> Dramix OL13/0.16 ( $L_f=13$  mm,  $d_f=0.16$  mm) steel fibres. The free opening between the strands and the mould was 16 mm. Table 1 shows the mixture composition; the volume of the superplasticiser is subtracted from the content of free water. The applied mixture is more expensive than the conventional concrete; due to the more slender shape of the sheet pile (less material) and other savings (production, placement of bar reinforcement, transport and faster construction) these costs are compensated.

Table 1: Mixture composition of SCFRC for sheet piles

Mixture composition	[kg/m <sup>3</sup> ]
CEM I 52.5 R	358
CEM III/A 52.5	555
Silica fume	61
Sand (0.125-0.5)	549
Sand (0.5-1.0)	549
Steel fibres (OL13/0.16)	125
Superplasticiser	(21)
Total water	226
w/c-ratio	0.25

The fibres are oriented along the flow due to the effect of the walls and the strands; especially in the lower flanges the flow distance was rather long. The fibres oriented along the flow in the lower flanges, whereas their orientation was more random in the upper flange [Tol, 2002]. The performance of the sheet piles in the hardened state was according to the

expectations, taking into account the orientation of the steel fibres and their effect on the tensile strength.

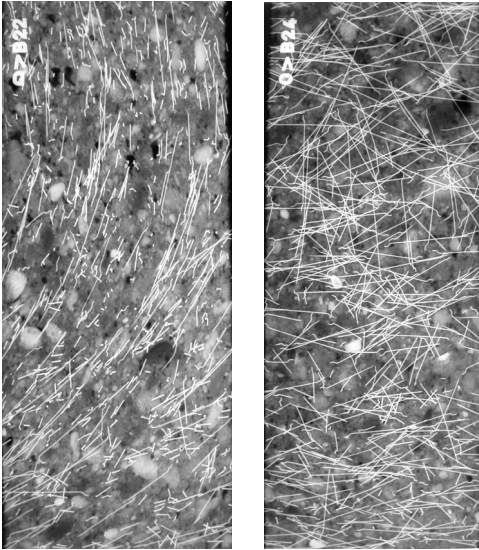
**Application: Tunnel segments**

Two tunnel segments were cast with SCFRC; two different types of steel fibres were applied (Dramix 80/60 BN;  $L_f/d_f = 80$ ,  $L_f = 60$  mm and Dramix 45/30 BN;  $L_f/d_f = 45$ ,  $L_f = 30$  mm). This project was carried out in cooperation with industrial partners: Strukton Group (Dutch contractor), Cementbouw (producer of ready-mix concrete) and Bekaert (producer of steel fibres). Each segment contained 60 kg/m<sup>3</sup> steel fibres. Table 2 shows the mixture composition.

*Table 2: Mixture composition of SCFRC for tunnel segments*

<i>Mixture composition</i>	<i>[kg/m<sup>3</sup>]</i>
CEM III 42.5 N	382
Fly ash	179
Sand (0.125-4 mm)	1044
Coarse aggregates (4-16 mm)	489
Water (incl. superplasticiser)	183
Superplasticiser LR	(2.43)
Superplasticiser HR	(1.17)
Steel fibres	60

Thirty cylinders were drilled from each segment, at different positions and in three directions. Deformation-controlled splitting tensile tests were executed on fifteen cylinders drilled from the first half of the segment, whereas X-ray photographs were taken of slices cut from cylinders taken from the second half of the segment. The orientation number is obtained by counting the fibres on the X-ray photographs [De Keukelaere, 1993]. The fibres were homogeneously distributed over the height of the cylinders; counting the fibres indicated that segregation did not occur. The X-ray photographs (Figures 19a and 19b) show the difference between two perpendicular directions with 60 mm fibres; the cylinders were drilled perpendicular to the upper side of the segments. More than three times more fibres crossed the plane (vertical line) within which the crack appears; consequently the splitting tensile strengths were rather different.



Figures 19 a/b: X-ray photographs: extreme orientation number (left: along the flow ( $\eta_\phi = 0.24$ ), right: perpendicular to the flow ( $\eta_\phi = 0.91$ ))

Figures 20 and 21 relate the orientation number with the splitting tensile strength, which is the maximum value of two strengths: when the first crack appeared or in the post-cracking stage.

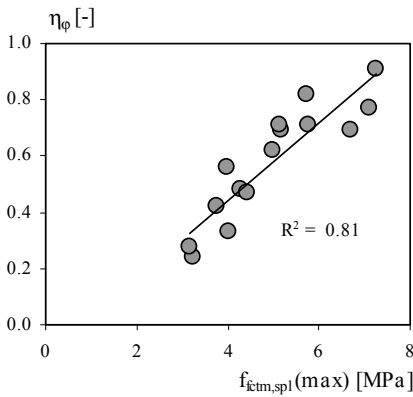


Figure 20: Splitting tensile strengths versus orientation numbers (tunnel segment with Dramix 80/60 BN steel fibres)

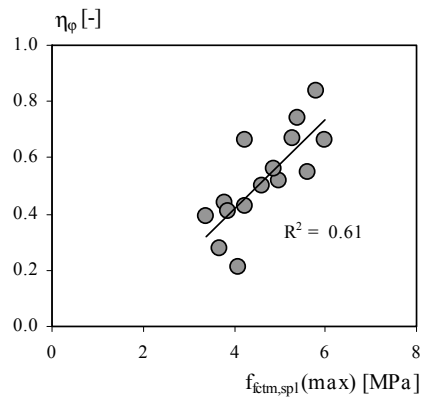


Figure 21: Splitting tensile strengths versus orientation numbers (tunnel segment with Dramix 45/30 BN steel fibres)

The test response depended on the position of the cylinders and on the direction in which they were tested. As Figures 20 and 21 show, the fibres are not randomly oriented in the tunnel segment; the flow affected the orientation of the fibres. The difference in orientation numbers of cylinders with 30 mm fibres was smaller (Figure 21). Consequently, the strengths differed less and the correlation between both parameters was lower. The orientation of the fibres was perpendicular rather than along the flow in the absence of walls. The reason was assigned to the production process of the tunnel segments. SCFRC flowed through the pipe of the truck mixer in the mould; the pipe was directed perpendicular to the longer side of the mould (Figure 22). During the flow through the pipe, its walls oriented the fibres. This effect was more pronounced for 60 mm fibres compared to 30 mm fibres. The concrete dropped vertically into the mould and distributed in a circular flow pattern. In the absence of walls the fibres were less oriented in the direction of the flow.



*Figure 22: Orientation of the pipe during casting and distribution pattern of SCFRC*

### **Application: Large beams**

The study on large beams aimed at investigating the effect of the flow and the fibre length on the orientation of the fibres. Two beams having a length of 3.7 m, a height of 0.5 m and a width of 0.2 m were cast with SCFRC. Figure 23 shows the position of different cross-sections cut from the beams. Two different types of steel fibres were applied: a 30 mm fibre (Dramix 45/30 BN) and a 50 mm fibre (Dramix 45/50 BN), which had the same aspect ratio ( $L_f/d_f$ ); the fibre content of each beam was 50 kg/m<sup>3</sup>. No bar reinforcement was arranged in the mould.

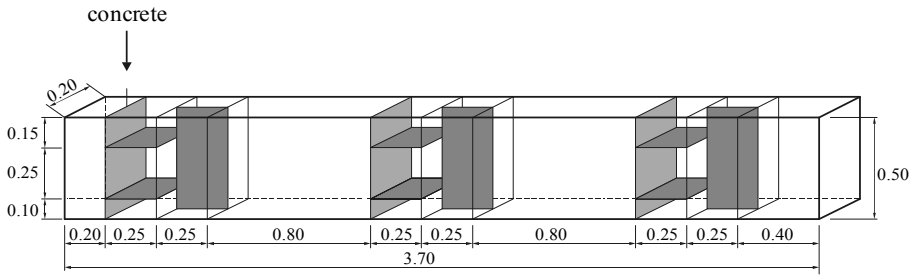


Figure 23: Test set-up: different directions and positions of the cross-sections

Digital photographs were taken from the cross-sections using a flashlight camera [Schönlin, 1988]. The orientation number of each cross-section was determined by applying an image analysis. The higher the orientation number (the average length of the fibres' cross-section in a plane decreases) the more the fibres are oriented perpendicular to the plane under consideration. Long steel fibres (50 mm) did orient parallel to the wall and from the vertical direction in the horizontal plane. Short fibres (30 mm) only oriented into the plane parallel to the wall, whereas the orientation number of the 30 mm fibres in the plane parallel to the bottom of the mould was almost constant along the flow; even a slight increase was observed. At increasing flow distance both fibre types aligned in the direction of the flow (Figure 24); the effect was more pronounced for 50 mm fibres. Short steel fibres were more randomly oriented even after a longer flow distance.

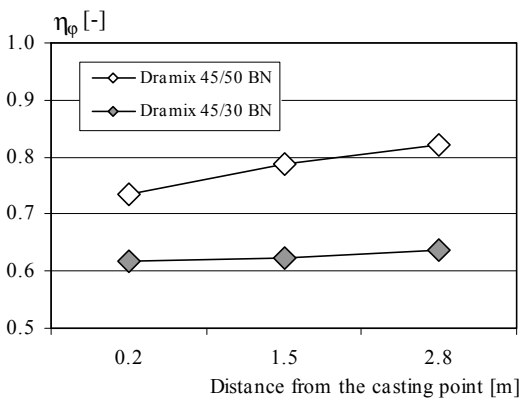


Figure 24: Orientation number of cross-sections perpendicular to the flow

## 5 Conclusions

SCFRC is an innovative type of concrete, which combines the advantages and extends the possibilities of both SCC and steel fibre reinforced concrete. A PhD-research was carried out at the Delft University of Technology to design and to optimise SCFRC. The thesis contains models that predict the performance of a wide range of mixture compositions and offers design tools that reduce the number of laboratory experiments required to obtain an optimised SCFRC. Based on the experimental studies and the analysis of the behaviour of SCFRC the following conclusions can be drawn:

- The addition of the steel fibres to a SCC affects the structure of the granular skeleton. The packing density decreases so a higher content of finer grains is required to compensate for it.
- Steel fibres affect the key characteristics of SCC. The applicable range of mixture compositions and characteristics in the fresh state of SCC containing high fibre contents (close to the maximum fibre content) is smaller compared to SCC.
- The performance of SCFRC in the hardened state depends on the direction in which a specimen is loaded. A comparison of the bending behaviour of SCFRC and SFRC indicated that SCFRC performed better and had a lower variation. The variation depends on the production process and the segregation resistance of SCFRC. The fibres are more oriented due to the walls of the mould and the flow when compared to SFRC.
- The production process might have a significant effect on the orientation of the fibres and the performance of SCFRC. The flow of SCFRC, once understood, is an effective tool to improve the efficiency of the fibres.

## Acknowledgements

The Dutch Technology Foundation STW and the Priority Program Materials (PPM) - research program 'Cement-Based Materials' (grant number 4010 III) - funded the project. They are gratefully acknowledged for their support.

## Literature

- Bartos, P.J.M., Sonebi, M., Tamimi, A. K. (2000): Workability and Rheology of Fresh Concrete: Compendium of Tests, Report of Technical Committee TC 145 WSM, Workability of Special Concrete Mixes, RILEM publications, Report 24, Cachan.
- Bui, V.K. (1994): A Method for the Optimum Proportioning of the Aggregate Phase of Highly Durable Vibration-Free Concrete, Master thesis, Asian Institute of Technology, Bangkok.
- CUR-Recommendation 70 (1999): Application of fly ash in mortar and concrete, CUR Gouda (in Dutch).
- De Keukelaere, G. (1993): Study on the distribution of fibres and their effect on mechanical characteristics of steel fiber reinforced concrete, Master thesis, Laboratory Magneel of Reinforced Concrete, University of Ghent, (in Dutch).
- Glavind, M. (1992): Evaluation of the compressive behaviour of fibre Reinforced High Strength Concrete, PhD-thesis, Department of Structural Engineering, Technical University of Denmark, Lyngby.
- Gopalaratnam, V.S., Shah, S.P. (1986): Strength, deformation and fracture toughness of fiber cement composites at different rates of flexural loading, Steel Fiber Concrete, US-Sweden Joint Seminar, Stockholm, Edited by Shah and Skarendahl, Elsevier Applied Science Publishers, New York, pp. 299-332.
- Grünewald, S. (2004): Performance-based design of self-compacting fibre reinforced concrete, PhD-thesis, Department of Structural and Building Engineering, Delft University of Technology, Delft University Press, Delft.
- Hordijk, D. (1991): Local approach to fatigue of concrete, PhD-thesis, Department of Structural and Building Engineering, Delft University of Technology.
- Johnston, C.D. (1996): Proportioning, mixing and placement of fibre-reinforced cements and concretes, Production Methods and Workability of Concrete, Edited by Bartos, Marrs and Cleland, E&FN Spon, London, pp. 155-179.
- Kooiman, A.G. (1998): Size-effect in the post-cracking behaviour of steel fibre reinforced concrete, Stevin-report 25.5-98-9, Department of Structural and Building Engineering, Delft University of Technology (in Dutch).
- Petersson, Ö., Billberg, P., Österberg, T. (1998): Applications of self compacting concrete for bridge castings, Second Int. Workshop on SCC, Kochi, Edited by Ozawa and Ouchi, Concrete Engineering Series, No. 30, Japan Society of Civil Engineers, pp. 318-327.

- Roelfstra, P.E., Wittmann, F.H. (1986): Numerical method to link strain softening with failure of concrete, *Fracture Toughness and Fracture Energy*, Edited by Wittmann, Elsevier, London.
- Schönlin, K. (1988): Determination of the orientation, the number and the distribution of fibers in fiber reinforced concrete, *Beton- und Stahlbetonbau* 83, No. 6, pp. 168-171 (in German).
- Tol, R. (2002): Sheet pile of high strength fiber reinforced self-compacting concrete - a design tested, Master thesis, Department of Structural and Building Engineering, Delft University of Technology (in Dutch).
- Vandewalle, L. (1993): Fibre reinforced concrete 'Special types of concrete and applications, Katholieke Universiteit Leuven, Departement Burgerlijke Bouwkunde,

## Appendix

The following equations (A1-A9) can be applied to calculate the parameters of the tensile model and to predict the bending behaviour of SCFRC:

$$f_{ictm,ax} = \frac{A - 0.465}{1.13} \quad (A1)$$

with:

$$A = \eta_{\phi} \cdot \left( (f_{ctm,spl} + (f_{ictm,spl} - f_{ctm,spl}) \cdot (V_f \cdot \frac{L_f}{d_f})) \right) \quad (A2)$$

in which

- $f_{ictm,ax}$  mean axial tensile strength of SFRC or SCFRC [MPa]  
 $f_{ictm,spl}$  mean splitting tensile strength of SFRC of SCFRC [MPa]  
 $f_{ctm,spl}$  mean splitting tensile strength of plain concrete [MPa]  
 $V_f \cdot L_f / d_f$  fibre factor [-]  
 $\eta_{\phi}$  orientation number [-]

$$w_0 = (0.187 + 3.52 \cdot 10^{-3} \cdot \frac{L_f}{d_f}) \cdot L_f \cdot \eta_{\phi} \quad (A3)$$

in which

- $w_0$  critical crack width [mm]

$L_f/d_f$  aspect ratio [-]  
 $L_f$  fibre length [mm]  
 $\eta_\phi$  orientation number [-]

$$w_c = \frac{0.494}{d_f} \cdot e^{0.0359 \cdot L_f} \quad (A4)$$

in which

$w_c$  characteristic crack width [mm]  
 $d_f$  fibre diameter [mm]  
 $L_f$  fibre length [mm]

$$f_{ictm,eq,bil} = MFF \cdot \eta_\phi \cdot FEF \quad (A5)$$

in which

$f_{ictm,eq,bil}$  mean equivalent post-cracking strength [MPa]  
 $MFF$  mechanical fibre factor (Equation A6) [MPa]  
 $\eta_\phi$  orientation number [-]  
 $FEF$  fibre efficiency factor (Table A1)[-]

with:

$$MFF = V_f \cdot \frac{L_f}{d_f} \cdot \alpha_f \quad (A6)$$

$$\alpha_f = PD_p \cdot \frac{\beta_f}{w/c} \quad (A7)$$

in which

$MFF$  mechanical fibre factor [MPa]  
 $V_f$  fibre content (volume) [Vol.-%]  
 $L_f/d_f$  aspect ratio [-]  
 $\alpha_f$  bond factor [MPa]  
 $PD_p$  packing density of paste [-]  
 $\beta_f$  factor incorporating the difference in shear stress of different fibre types [MPa],

(1.9 MPa for straight and 2.1 MPa for hooked-end steel fibres [Glavind, 1992])

$w/c$  water-cement ratio / water-binder ratio [CUR-Recommendation 70, 1999] [-]

Table A1: Fibre efficiency factors (FEF) of hooked-end steel fibres

<i>Fibre type</i>	<i>Fibre efficiency factor</i>
Dramix 80/60 BP	0.873
Dramix 80/30 BP	0.745
Dramix 45/30 BN	0.912
Dramix 65/40 BN	0.625

$$\epsilon_{ct, \text{fibre}} = 0.184 \cdot 10^{-3} \left( \frac{L_f}{d_f} \right)^{2.31} \quad (\text{A8})$$

in which

$\epsilon_{ct, \text{fibre}}$  reduced elastic strain of SCFRC in tension [‰]

$L_f/d_f$  aspect ratio [-]

$$s \cdot f_{ctm, ax} = 0.40 \cdot f_{ctm, spl} \quad (\text{A9})$$

in which

$s \cdot f_{ctm, ax}$  mean axial tensile strength of SCFRC at first cracking [MPa]

$f_{ctm, spl}$  mean splitting tensile strength of SFRC of SCFRC [MPa]

